



Published in final edited form as:

J Immunol. 2010 April 1; 184(7): 3927–3936. doi:10.4049/jimmunol.0903475.

Fatty acids from VLDL lipolysis products induce lipid droplet accumulation in human monocytes

Laura J den Hartigh^{†,‡,||}, Jaime E Connolly-Rohrbach^{†,§,||}, Samantha Fore^{†,¶}, Thomas R Huser^{†,¶}, and John C Rutledge[†]

[†]Department of Internal Medicine, Division of Endocrinology, Clinical Nutrition, and Vascular Medicine, University of California, Davis, CA 95616

[‡]Department of Veterinary Medicine, Division of Pathology, Microbiology, and Immunology, University of California, Davis, CA 95616

[§]Department of Cell Biology and Human Anatomy, University of California, Davis, CA 95616

[¶]Center for Biophotonics Science and Technology, University of California, Davis, CA 95616

Abstract

One mechanism by which monocytes become activated postprandially is by exposure to triglyceride (TG)-rich lipoproteins such as very low-density lipoproteins (VLDL). VLDL are hydrolyzed by lipoprotein lipase (LpL) at the blood-endothelial cell interface, releasing free fatty acids. In this study, we examined postprandial monocyte activation in more detail, and found that lipolysis products generated from postprandial VLDL induce the formation of lipid-filled droplets within cultured THP-1 monocytes, characterized by coherent anti-stokes Raman spectroscopy. Organelle-specific stains revealed an association of lipid droplets with the endoplasmic reticulum, confirmed by electron microscopy. Lipid droplet formation was reduced when LpL-released fatty acids were bound by bovine serum albumin, which also reduced cellular inflammation. Furthermore, saturated fatty acids induced more lipid droplet formation in monocytes compared to mono- and polyunsaturated fatty acids. Monocytes treated with postprandial VLDL lipolysis products contained lipid droplets with more intense saturated Raman spectroscopic signals than monocytes treated with fasting VLDL lipolysis products. In addition, we found that human monocytes isolated during the peak postprandial period contain more lipid droplets compared to those from the fasting state, signifying that their development is not limited to cultured cells but also occurs *in vivo*. In summary, circulating free fatty acids can mediate lipid droplet formation in monocytes and potentially be used as a biomarker to assess an individual's risk of developing atherosclerotic cardiovascular disease.

Keywords

atherosclerosis; lipid droplets; free fatty acids; postprandial state; lipotoxicity; transmission electron microscopy; endoplasmic reticulum; coherent anti-stokes Raman spectroscopy

Introduction

Understanding interactions between circulating monocytes and lipoproteins is currently an area of active investigation related to inflammatory diseases such as atherosclerosis (1,2).

Corresponding author: Laura J den Hartigh, University of California, Davis, VM3A room 4206, One Shields Avenue, Davis, CA 95616, Phone: 530-754-8714, Fax: 530-752-3349, ljhiggins@ucdavis.edu.

^{||}These authors contributed equally to this work.

Triglyceride-rich lipoproteins, such as VLDL, are commonly regarded as pro-inflammatory (3). VLDL, which are generated by the liver, are hydrolyzed by LpL anchored to endothelial cells, resulting in the release of free fatty acids, phospholipids, monoglycerides, and diglycerides and the conversion of VLDL into remnant lipoproteins. This process is enhanced postprandially and can induce cellular injury in neighboring endothelial cells and monocytes (4). Such inflammatory injury can result in increased monocyte activation and recruitment to the arterial intima, contributing to foam cell development and fatty streak formation characteristic of atherosclerotic cardiovascular disease (ASCVD).

Excessive lipid accumulation within cells is a central feature of some metabolic diseases such as atherosclerosis, but little is known about the role that cytoplasmic lipid droplets play in monocyte responses to hypertriglyceridemia. Lipid droplets are commonly found in adipocytes, but exist in virtually all types of cells when faced with lipid overload. In non-adipocytes, lipid droplets are believed to function as lipid storage sites for later beta-oxidation, membrane biogenesis, hormone synthesis, and other cellular functions (5). Recently, more diverse functions of the lipid droplet have been discovered largely related to intracellular signaling, protein storage, as well as protein degradation (6–9). Lipid droplets typically consist of a core of neutral lipids comprised of triglycerides, cholesterol esters, and fatty acids, surrounded by a phospholipid monolayer (10,11). It has been suggested that lipid droplets originate from the endoplasmic reticulum (ER), as they have been found in close proximity to ER membranes and contain a similar phospholipid profile as the ER (12,13). The molecular composition, cell-specific function, and biogenesis of the lipid droplet are intense areas of investigation and currently remain unknown.

Prevention of lipid overload may be important in the prevention of metabolic disease states. A new unified view of lipid droplets as distinct organelles with the ability to store excess lipids and to participate in specific intracellular signaling cascades related to the energy requirements of the cell (14), makes them attractive targets for investigation. In this study, monocyte treatment with VLDL lipolysis products generated by treating VLDL with LpL resulted in the formation of cytoplasmic lipid structures, which led us to examine their origins in more detail. We determined that the droplets were indeed lipid-filled and that fatty acids were partially responsible for this lipid droplet formation. In addition, there appears to be a correlation between VLDL lipolysis product-induced cytokine synthesis and lipid droplet formation. Organelle-specific stains indicated that in monocytes, as has been observed in other cell types, the lipid droplets associate with the ER, a finding we confirmed by transmission electron microscopy (TEM). Furthermore, monocyte treatment with postprandial VLDL lipolysis products resulted in the formation of lipid droplets with more intense saturated Raman spectroscopic modes, while fasting VLDL lipolysis product-treated monocytes contained lipid droplets exhibiting higher unsaturated lipid modes. Similar lipid droplets were found in fresh human monocytes isolated from postprandial whole blood. Our study presents novel observations that lipolysis products generated from VLDL induce the rapid formation of cytoplasmic lipid droplets within naïve monocytes *in vitro*, and freshly isolated primary postprandial monocytes contain similar lipid structures, observations that may be clinically important. Thus, lipid droplet formation by postprandially-activated monocytes appears to be a potential mechanism of lipotoxic protection but additionally results in monocyte inflammation, which has been linked to vascular inflammation and ASCVD.

Materials and Methods

Monocyte Cell Culture and Treatment Conditions

THP-1 human monocytes were purchased from American Type Culture Collection and maintained in suspension between 5×10^4 and 8×10^5 cells/ml in RPMI 1640 medium supplemented with 2 mM L-glutamine and containing 10 mM HEPES (4-(2-hydroxyethyl)-1-

piperazineethanesulfonic acid), 1 mM sodium pyruvate, 4.5 g/L glucose, 1.5 g/L bicarbonate, 10% fetal bovine serum, and 0.05 mM 2-mercaptoethanol. Monocytes were incubated in 5% CO₂ and 95% O₂ at 37°C during growth and treatment. THP-1 monocyte treatments were conducted at a cell density of 1 × 10⁶ cells/ml for the times indicated. Monocyte viability was monitored after all treatments using trypan blue exclusion, and remained above 90% for all treatments. Prior to cell treatment, lipolysis of VLDL was performed by incubating VLDL (200 mg TG/dL) with bovine LpL (2 U/mL, Sigma-Aldrich) for 30 minutes at 37°C. In some experiments, fatty-acid free BSA (60 mg/mL, Sigma-Aldrich) was added to each lipid treatment 5 minutes prior to exposure to the cells. In other experiments, THP-1 cells were treated with the synthetic fatty acids linoleic acid (Cayman Chemicals), oleic acid (Sigma-Aldrich), stearic acid (Cayman Chemical), and palmitic acid (Nu-Check Prep), at 150 μM each, for 3 hours. In all experiments, THP-1 monocytes were treated at a cell density of 1 × 10⁶ cells/mL for the times indicated. Lipid droplets were confirmed by differential interference contrast (DIC) microscopy using a 40× objective or phase contrast microscopy using a 60× objective. For some experiments, human peripheral blood mononuclear cells (PBMC) were isolated by centrifuging buffy coats over a Lymphosep density solution (ρ = 1.07, MP Biomedical) for 20 minutes, washed 3 times, and immediately processed for quantitative RT-PCR. All THP-1 monocytes, freshly isolated human monocytes, and PBMC used in these experiments were maintained in an undifferentiated state.

Very Low-Density Lipoprotein Isolation

Male and female healthy human volunteers ages 18–55 were recruited from the University of California, Davis campus. The study was approved by the Human Subjects Research Committee of the University of California, Davis. The study aims and protocol were explained to each participant and informed written consent was obtained. All studies were performed at the same time of day to eliminate any diurnal variables. Blood was drawn by venipuncture from subjects before and 3.5 hours following consumption of a moderately high fat meal (40% calories from fat, as described previously (3)) into K₂-EDTA (ethylenediaminetetraacetic acid) vacutainer tubes and centrifuged at 1,200g for 10 minutes to obtain cell-free plasma. Plasma was treated with 0.01% sodium azide as a preservative and subjected to lipoprotein isolation as described previously (15), with minor modifications. Chylomicrons were removed from postprandial plasma by centrifuging for 30 minutes at 63,000g prior to VLDL isolation. VLDL samples from multiple donors were pooled together and dialyzed overnight at 4°C in 0.9% NaCl (sodium chloride) and 0.01% EDTA and quantified for total triglyceride content using a kit from Sigma-Aldrich. Lipolysis of VLDL was induced by the addition of bovine lipoprotein lipase (LpL, Sigma-Aldrich) at 2 Units/mL for 30 minutes at 37°C, where indicated.

Oil Red O Staining

THP-1 human monocytes (1 × 10⁶ cells/ml) were treated with VLDL (200 mg TG/dl), LpL (2 U/mL) or VLDL lipolysis products generated as described above for 3 hours at 37°C. Cells were harvested following treatment, washed one time with phosphate buffered saline without calcium chloride and magnesium chloride, and resuspended in 1% paraformaldehyde for fixation. Following incubation at room temperature for 30 minutes, the cells were collected, washed one time with deionized water, and resuspended in 60% isopropanol for 5 minutes. The isopropanol was removed, the cells were resuspended in Oil Red O stain (Lonza Walkersville, Inc., Switzerland), and incubated at room temperature for 5 minutes. Following staining, the cells were washed several times with deionized water to remove excess stain, resuspended in 20 μl deionized water and viewed using DIC, phase contrast, or epifluorescence microscopy.

CARS Imaging of Monocyte Lipid Droplets

To analyze lipid-filled droplets in living monocytes, we utilized a custom-built coherent anti-Stokes Raman scattering (CARS) microscopy system. A 1064 nm Nd:YVO₄ laser (PicoTrain, HighQ Laser) with 7ps pulse width and 76 MHz repetition rate is used as the Stokes pulse to generate the CARS signal and also serves as the pump laser for an Optical Parametric Oscillator (OPO, Levante, APE-Berlin). The tunable OPO with a wavelength range between 790 nm – 920 nm provides the pump pulse for the CARS signal generation. Both beams are spatially and temporally overlapped and combined by a 970 nm dichroic mirror. To diminish potential photo damage to the cells, the laser repetition rate is reduced tenfold to 7.6 MHz by an electro-optical modulator (Conoptics). The combined laser beams are sent into an inverted optical microscope (I×71, Olympus) and focused to a diffraction-limited spot by a 60× oil objective (Olympus America, Center Valley, PA). The forward-directed CARS signal generated in the sample is separated from the laser beams by a dichroic mirror and a multiphoton short-pass filter (Semrock) and is then collected by a single photon counting avalanche photodiode detector (APD, SPCM-AQR 14, Perkin-Elmer). The APD signal is processed using time-correlated single photon counting electronics (TimeHarp200, PicoQuant GmbH) and displayed using image acquisition and analysis software (SymPhoTime, PicoQuant GmbH).

To image lipid droplets in primary monocytes, the OPO beam was tuned to 816 nm and serves as the pump laser, while the 1064 nm line of the Nd:YVO₄ laser was used as the Stokes probe beam. Together, the two beams coherently probe the strong aliphatic lipid CH stretch vibration at 2854 cm⁻¹, which results in the generation of a strong CARS signal at 661 nm. Images are acquired at 256×256 pixels with an acquisition time of 1 min/image.

In vitro LysoTracker, MitoTracker, and ER-Tracker Analysis

THP-1 human monocytes (1×10^6 cells/mL) were treated with VLDL lipolysis products generated as described above for 3 hours at 37°C. Following treatment, cells were stained with LysoTracker Red DND-99 (50 nM final concentration; Molecular Probes), MitoTracker Green FM (50 nM final concentration; Molecular Probes), or ER-Tracker Red (100 nM final concentration; Molecular Probes). Cells stained with ER-Tracker Red were then fixed in 1% paraformaldehyde for 2 minutes at 37°C, washed, and resuspended in 20 µl probe-free medium. Localization of the Tracker dyes was examined by fluorescein isothiocyanate or rhodamine optical filters on a Zeiss Axioskop 2 plus fluorescence microscope.

Transmission Electron Microscopy (TEM)

THP-1 human monocytes (1×10^6 cells/ml) were treated with VLDL lipolysis products generated as described above for either 30 minutes or 3 hours at 37°C. At each time point, 1 mL of cells were harvested and fixed by resuspension in modified Karnovsky's fixative (2% paraformaldehyde and 2.5% glutaraldehyde in 0.06 M Sorenson's phosphate buffer, pH 7.2). Cells were washed in Sorenson's phosphate buffer three times for one minute each, resuspended in 2% OSO₄ (osmium tetroxide), and incubated at 4°C for one hour. Prior to dehydration, the cells were washed in distilled water three times for one minute each at 4°C. Samples were dehydrated through serial washes in graded acetone (10 minutes each). The dehydrated samples were embedded in epoxy resin and ultra thin sections were obtained after heavy metal staining. The images were collected on a Phillips CM120 microscope at 80kV.

Quantitative real-time Reverse Transcription Polymerase Chain Reaction (qRT-PCR)

Gene expression of inflammatory cytokines from treated monocytes was examined using qRT-PCR as described previously (16). Briefly, RNA was extracted from treated THP-1 cells using TRIzol reagent (Invitrogen) and an RNeasy mini kit (Qiagen). 5 µg total RNA was converted to cDNA using a Superscript III kit (Invitrogen). Quantification of mRNA from gene transcripts

of tumor necrosis factor alpha (TNF α), interleukin 1 beta (IL-1 β), interleukin 8 (IL-8), and beta-actin was performed using the GeneAmp 7900 HT sequence detection system (Applied Biosciences), as described previously (17). Primers for the genes of interest were designed using Primer Express (Applied Biosystems) and synthesized by Integrated DNA Technologies. The primer sequences were as follows: TNF α (sense, 5'-AACATCCAACCTTCCCAAACG-3'; antisense, 5'-CCCTAAGCCCCCAATTCTCTT-3'), IL-1 β (sense, 5'-AATTTGAGTCTGCCAGTTCCC-3'; antisense, 5'-AGTCAGTTATATCCTGGCCGCC-3'), IL-8 (sense, 5'-GAGAAATCAGGAAGGCTGCC-3'; antisense, 5'-ACATGACTTCCAAGCTGGCC-3'), and beta-actin (sense, 5'-CTGTCCACCTCCAGCAGATGT-3'; antisense, 5'-CGCAACTAAGTCATAGTCCGCC-3'). Expression of TNF α , IL-1 β , and IL-8 were normalized to beta-actin and represented in terms of a fold change.

TNF α ELISA

Secreted TNF α protein from treated THP-1 monocytes was quantified using a human ELISA kit, according to the manufacturer's instructions (BD Biosciences).

Spontaneous Raman Spectroscopy of Single Lipid Droplets in Monocytes

Spontaneous Raman spectra of single lipid droplets within monocytes were acquired on a custom-built inverted laser-tweezers Raman microscope. The main microscope platform consists of an Olympus IX-71 microscope equipped with a 100 \times , NA 1.4, oil immersion objective optimized for near-IR operation (Olympus America, Center Valley, PA). The laser source is an 80 mW, 785 nm diode-pumped solid-state laser (Crystalaser, Reno, NV). The spontaneously scattered Raman-shifted light is collected by the same microscope objective, dispersed by an imaging spectrograph (SP2300i, Roper Scientific, Trenton, NJ), equipped with a 300 lines/mm grating, and detected with a back-illuminated, thermoelectrically-cooled depletion charge-coupled device (CCD) camera with 1340 \times 1000 pixels (PIXIS 100BR, Roper Scientific, Trenton, NJ). To acquire spectra from individual lipid droplets in monocytes, the monocytes were optically trapped by their cytoplasmic lipid droplets utilizing the highly focused near-infrared laser beam. This immobilizes the cell and allows us to obtain full Raman spectra within 30–60 sec signal acquisition time. Background spectra were acquired from the buffer solution, while avoiding trapping any cells. After the subtraction of the individual background spectra, the resulting spectra were processed equally, including baseline subtraction and peak area normalization.

Analysis of Lipid Droplets in Human Monocytes

Buffy coats were isolated from blood drawn during the fasting and peak postprandial periods. Contaminating erythrocytes were removed using a lysing solution (BD Biosciences). Monocytes within the buffy coats were labeled with an Alexa488-conjugated CD14 antibody, cells were fixed using 1% paraformaldehyde, and then stained with Oil Red O as described above. Cells were imaged with a personal DV deconvolution microscope (Applied Precision, LLC, Issaquah, WA) using a 40 \times objective. A FITC filter was used for excitation of the Alexa-488 and Oil Red O, and emission profiles at 528 nm and 617 nm were used to detect CD14 and Oil Red O, respectively. A minimum of 40 frames of cells were captured per sample. Images were deconvolved using Delta Vision software, giving a partially computer-generated final image. Total monocytes with and without lipid droplets were counted from samples isolated from the fasting state and the peak postprandial period, and presented as a percentage of monocytes positive for lipid droplets. Additionally, total triglycerides and non-esterified fatty acids were measured from the corresponding plasma samples using kits from Sigma-Aldrich and Wako Chemicals, respectively, according to the manufacturer's instructions.

Statistics

All statistical analyses were performed using student's t-test or one-way ANOVA, where appropriate, with SigmaStat software. All data are presented as the mean \pm standard error of the mean (SEM). Statistical significance was reported for $P < 0.05$.

Results

Treatment of THP-1 monocytic cells with VLDL lipolysis products induces lipid droplet biogenesis

Initial studies revealed that THP-1 cells develop intracellular droplet-like structures following a 3-hour treatment with VLDL lipolysis products, generated by pre-treating VLDL with LpL. DIC microscopy was used to visualize the droplet-like structures in the VLDL lipolysis product-treated cells (Figure 1D, arrows). Cells were stained with Oil Red O, which stains neutral lipids, to confirm that the droplets are lipid-filled. Untreated THP-1 monocytes (Figure 1A) and monocytes treated with LpL (Figure 1B) or VLDL alone (Figure 1C) contained very few droplets. Supplemental Figure S1 represents DIC microscopic images of treated cells without Oil Red O staining, to confirm that the lipid droplet formation is not an artifact of the Oil Red O staining procedure.

To further confirm that lipid-filled droplets exist in living monocytes and to avoid potential artifacts from fixation or Oil Red O staining, we also imaged treated THP-1 monocytes by CARS microscopy. CARS microscopy is a label-free chemical imaging technique suitable for live cell microscopy that probes specific molecular vibrations by inelastic light scattering. Here, we tuned our system to probe the aliphatic CH vibration at 2845 cm^{-1} that is common to all lipids (Figure 2A). Images obtained by this technique are similar to confocal fluorescence microscopy images, but are based on the intrinsic contrast between these specific molecular vibrations. As shown in the CARS image in Figure 2B, only lipid droplets within the cytoplasm of a monocyte produce visible contrast using this modality, which further underscores the highly localized lipid storage in these cells. The lipid droplets imaged in this cell are all of approximately the same size and similar overall lipid density.

VLDL lipolysis product-induced lipid droplets appear to be in close proximity to the ER

Lipid droplets can form within cells by several processes, but they most commonly originate from the ER. To determine if VLDL lipolysis product-induced lipid droplets are associated with ER structures, treated monocytes were stained with ER-Tracker Red and observed at various time points over a course of 3 hours (Figure 3). THP-1 cells treated with VLDL lipolysis products (200 mg TG/dL VLDL + 2 U/mL LpL) between 0.5 and 3 hours show the gradual accumulation of lipid droplets within the cells, with the greatest number of lipid droplets observed by 3 hours clearly seen by DIC (Figure 3A, first column). ER-Tracker Red dye (Figure 3A, middle column) displays a punctate cytoplasmic localization early in the time course (0.5–1 hour), consistent with ER localization. As lipid droplets form, most noticeably at 2 and 3 hours, they appear to associate with ER membranes (white arrows). Specifically, at 2 hours, you can see that the ER-Tracker Red dye is largely localized to one area where a lipid droplet is located within the cell. By 3 hours, the ER-Tracker Red dye appears to surround the periphery of the lipid droplet and is highly concentrated in close proximity to one side of the lipid droplet. This finding is consistent with the idea that neutral lipids coalesce within the ER bilayer into a sphere that eventually buds into the cytosol, a model largely accepted in the lipid droplet field, but is nonetheless unproven (18). A merge of the two images is presented in Figure 3A.

To determine if other cellular organelles could be involved in lipid droplet biosynthesis, VLDL lipolysis product-treated THP-1 monocytes were stained with Lyso-Tracker Red DND-99 (Supplemental Figure S2B) and Mito-Tracker Green FM (Supplemental Figure S2E) to stain

lysosomes and mitochondria, respectively. Neither stain appeared to strongly co-localize with the lipid droplets (Supplemental Figure S2C and S2F, black arrows), suggesting that these structures are not involved in lipid droplet formation.

To further investigate the cellular origin of the lipid droplets and confirm their association with the ER, we examined thin sections of VLDL lipolysis product-treated THP-1 monocytes by TEM after 0.5 and 3 hours. Figure 3B shows that small lipid droplets (arrows) are visible as early as 30 minutes following treatment (8510 \times total magnification). After 3 hours, the droplets appear to be larger in size (Figure 3C, 8510 \times total magnification), perhaps due to fusion of multiple smaller droplets within the cell. However, the mechanism that results in this increase in droplet size remains to be elucidated (18). Increased magnification revealed that the lipid droplets are indeed variable in size after 3 hours of lipolysis product treatment (Figure 3D, 15900 \times total magnification), and TEM confirms that the lipid droplets are found opposed to the ER, which supports the idea that the lipid droplets likely bud off from the ER during their generation (Figure 3E, 11000 \times total magnification).

Albumin binding to fatty acids released from lipolysis of VLDL attenuates lipid droplet formation and cytokine expression

To determine if fatty acids released from hydrolysis of VLDL are involved in lipid droplet formation in THP-1 monocytes, we used fatty acid-free BSA to sequester the fatty acids prior to monocyte treatment. Following a 2-hour treatment, monocytes were stained with Oil Red O and counted as positive or negative for lipid droplets by phase contrast microscopy. Figure 4A shows that less than 10% of untreated monocytes contained lipid droplets. Adding BSA to the untreated culture medium had no effect on lipid droplet formation. Treatment with LpL or VLDL, negative controls, did not result in a significant change in lipid droplet formation with or without BSA. However, 80% of monocytes treated with VLDL lipolysis products contained lipid droplets, a significant increase from the controls. Allowing BSA to bind to fatty acids released from the lipolysis of VLDL significantly decreased the number of lipid droplet-laden monocytes (50%, $P < 0.05$), suggesting that free fatty acids, unbound to albumin, play an important role in lipid droplet formation in THP-1 monocytic cells.

Another consequence of monocyte treatment with VLDL lipolysis products was increased cytokine expression. A natural monocytic response to pathogens or toxins is the release of cytokines and chemokines, to ultimately mount an acute inflammatory defense. Such monocyte activation by non-foreign stimuli, such as modified lipids, has been described as an initiating event in atherogenesis (19–21). Figure 4B illustrates that TNF α , IL-1 β , and IL-8 gene expression significantly increased in THP-1 cells after lipolysis product treatment. Furthermore, sequestering lipolytically released fatty acids with BSA, and therefore reducing the number of lipid droplets within the cell, attenuated this cytokine expression. This observation suggests that lipid overload within the cell triggers inflammatory signaling pathways that could result in cellular activation.

Additionally, to ensure that our treatment time of 3 hours adequately represented the inflammation induced postprandially, TNF α protein secretion from THP-1 monocytes treated with VLDL lipolysis products for 3, 6, and 24 hours was measured by ELISA. The highest secreted TNF α protein levels were observed after 3 hours (86.4 pg/mL vs. 65.4 and 62.2 pg/mL after 6 and 24 hours, respectively), confirming that our *in vitro* replication of the peak postprandial period is accurate (data not shown).

Synthetic fatty acids induce lipid droplet formation

Lipolysis of VLDL results in the release of large quantities of non-esterified fatty acids (22), which have the potential to affect monocytes through a variety of mechanisms. To confirm that

fatty acids induce lipid droplet formation, THP-1 monocytes were treated with commercially available unsaturated fatty acids (linoleic acid- 18:2 $n-6$, and oleic acid- 18:1), and saturated fatty acids (stearic acid- 18:0, and palmitic acid- 16:0). The treatment medium also contained 10% serum albumin. Monocytes were observed under phase contrast microscopy after treatment with 150 μM of each fatty acid, which is within the physiological range of non-esterified fatty acids for humans (23). Lipid droplets were abundant in monocytes treated with each fatty acid as seen in Figure 5. Linoleic acid (Figure 5A), oleic acid (Figure 5B), and stearic acid (Figure 5C) treatment resulted in the lowest incidence of droplet formation with 53.9%, 50.4%, and 57.8% of total monocytes displaying lipid droplets, respectively, represented quantitatively in Figure 5E. Palmitic acid treatment ultimately generated the highest percentage of lipid droplet-containing cells (Figure 5D, 76.9%), and the droplets that formed within palmitic acid-treated monocytes appeared larger in size than droplets inside cells from any other treatment. This higher incidence of lipid droplet formation from palmitic acid treatment was found to be statistically significant ($P < 0.05$).

Interactions with lipolysis products from fasting or postprandial VLDL change the lipid composition of lipid droplets

To determine whether lipolysis products from fasting VLDL or postprandial VLDL have an influence on the lipid composition of monocyte droplets, we acquired Raman spectra from lipid droplets across the entire Raman-active range from $\sim 400\text{ cm}^{-1}$ to 3100 cm^{-1} utilizing a laser tweezers Raman microscope. This instrument allows us to optically trap monocytes in culture by their cytoplasmic lipid droplets, thereby immobilizing the lipid droplet in the tightly focused laser spot for the duration of the experiment (typically 30–60 seconds per lipid droplet). In Figure 6, we show Raman spectra representing the average of several lipid droplets from monocytes that underwent each treatment. All spectra are dominated by the vibrational signature of lipids, indicating that the monocytes were indeed trapped by their lipid droplets. These peaks correspond to the following assignments: Raman peaks of acyl chains in the $1000\text{--}1200\text{ cm}^{-1}$ range are typically due to C-C stretching vibration. Specifically, peaks at 1066 , 1076 , and 1129 cm^{-1} are known to be very sensitive indicators of acyl chain order in lipids. These peaks usually indicate close chain packing typical of the structure of saturated fatty acids at room temperature.

To quantitatively analyze the lipid contents of these droplets, we normalized all the peak vibrations to the 1442 cm^{-1} CH deformation mode, which indicates total lipid content. Specifically, recent papers have established that the ratio of the peak intensity of the 1654 cm^{-1} C=C stretch mode to the 1442 cm^{-1} general lipid vibration provides an excellent quantitative measure of the degree of unsaturation in intracellular lipid droplets (24–26). By carefully comparing these modes between the different samples, it can be seen that monocytes treated with postprandial VLDL have an elevated intensity at the 1129 cm^{-1} mode (I_{1129}/I_{1445} : PVLVDL: 0.16 ± 0.01 , FVLVDL: 0.08 ± 0.01 , PVLVDL+LpL: 0.11 ± 0.01 , FVLVDL+LpL: 0.08 ± 0.01). This ratio is similar to that obtained directly from postprandial VLDL lipoproteins and indicates that their saturated fatty acid core is likely being incorporated in its entirety into intracellular lipid droplets (24). Interestingly, the observation is quite different when the total degree of unsaturation is calculated (ratio I_{1654}/I_{1445} : PVLVDL: 0.46 ± 0.04 , FVLVDL: 0.50 ± 0.04 , PVLVDL+LpL: 0.57 ± 0.05 , FVLVDL+LpL: 0.65 ± 0.05). Here, treatment with lipolysis products leads to significantly higher degrees of unsaturation, suggesting that monocytes are trying to compensate the lipotoxic effects of exposure to saturated fatty acids. Interestingly, the triglyceride content in all cells is relatively unchanged and rather similar (ratio I_{1740}/I_{1445} : PVLVDL: 0.08 ± 0.01 , FVLVDL: 0.07 ± 0.01 , PVLVDL+LpL: 0.11 ± 0.01 , FVLVDL+LpL: 0.12 ± 0.01). Based on these observations it is quite apparent that lipid droplets in monocytes treated with postprandial VLDL lipolysis products contain on average about 15% more saturated lipids than those from fasting VLDL lipolysis product-treated monocytes.

Lipid droplets are present in primary human monocytes after consumption of a high fat meal

To eliminate the possibility that the cytotoxic response of THP-1 monocytes to VLDL lipolysis products is an *in vitro* effect, we examined freshly isolated human monocytes before and after the consumption of a moderately high fat meal. Monocytes were labeled with a CD14 antibody, a cell surface marker found exclusively on monocytes, conjugated to the fluorescent dye Alexa488 that renders all monocytes fluorescent green. Monocytes were fixed and subsequently stained with Oil Red O for lipid droplet visualization at red wavelengths. Monocytes isolated from fasting blood contained few red-stained lipid droplets (Figure 7A), while cells isolated from postprandial blood contained more lipid droplet-positive monocytes (Figure 7B). Monocytes positive for lipid droplets, i.e. cells that stained green and contained punctate red droplets, were counted and expressed as a percentage of total monocytes. In this study comparing the responses of 10 randomly selected healthy volunteers, 29.4% of fasting monocytes contained lipid droplets, compared to 50.3% of postprandial monocytes (Figure 7C). Similarly, when THP-1 monocytes were treated with fasting or postprandial plasma at the same average triglyceride concentrations expressed by our donors (42 and 79 mg TG/dL, respectively), the percentage of cells positive for lipid droplets (33.5% fasting and 70.0% postprandial, data not shown) closely mimicked the trend observed using fresh monocytes. The red cells in Figure 7A are non-monocytic leukocytes that have picked up the Oil Red O stain. Note that most of these cells are uniformly stained red, with few punctate red spots, suggesting that Oil Red O stains plasma membrane lipids of all cells. However, in Figure 7A there are a few non-monocytic leukocytes that stain brightly red in a speckled pattern, which suggests that some unidentified non-monocytic leukocytes also develop lipid droplets. In Figure 7B, we believe that the absence of red non-monocytic leukocytes is due to the chosen focal plane in this particular frame, in which the monocytes are in focus and the underlying non-monocytic leukocytes are below the plane of focus. This, and the brightness of the red droplets within the monocytes, renders the Oil Red O signal from the nonmonocytic leukocytes slightly dampened.

Since the postprandial period chosen coincides with the average spike in triglycerides seen following ingestion of a high fat meal, as shown in Figure 7D, it appears that circulating triglycerides or their lipolysis products induce lipid droplet formation within monocytes *in vivo*. The average non-esterified fatty acid (NEFA) levels of the fasting and postprandial plasma were 0.242 mmol/L and 0.301 mmol/L, respectively. In addition, the 10 blood donors had an average postprandial triglyceride level of 79 mg/dL. Since this value is lower than the triglyceride levels used in our previous treatments, we repeated the initial THP-1 monocyte treatment with VLDL lipolysis products at this triglyceride concentration (data not shown). The loading capacity at 79 mg TG/dL was quantified as 69% of total THP-1 monocytes containing lipid droplets, slightly lower than the 200 mg/dL dose depicted in Figure 4 (80% positive for droplets).

As an additional link to monocyte inflammation, a previous study from our lab showed that the peak postprandial period also coincided with increased levels of TNF α and IL-1 β secretion from circulating monocytes (3). To confirm that lipid droplet formation in fresh monocytes also correlates with an inflammatory response, we isolated peripheral blood mononuclear cells (PBMC) from fasting and 3.5-hour postprandial blood and measured cytokine gene expression. As shown in Supplemental Figure S3, PBMC expression levels of TNF α , IL-1 β , and IL-8 significantly increased during the peak postprandial period, confirming our previous observation.

Discussion

The aims of this study were to identify and characterize the cytosolic lipid droplets that form in monocytes in response to incubation with lipolysis products from VLDL and to determine how this effect relates to postprandial hypertriglyceridemia. Controlled lipid storage is a known

function of monocyte-derived macrophages, but to our knowledge has not been investigated in undifferentiated monocytes. We found that monocytes in culture and freshly isolated primary monocytes display similar lipid droplet formation when exposed to postprandial VLDL lipolysis products, suggesting that this is not an artifact of cell culture or unique to a particular cell line. Fatty acids released upon lipolysis appear to be causative, and the level of unsaturation of these fatty acids is critical for their rate of formation and the size to which the droplets can grow. Furthermore, these lipid droplets appear to originate from the ER as previously suggested, in agreement with the current lipid droplet model.

Lipid droplet physiology has been the subject of intense research for many years, but gaps in the knowledge base remain. Specifically, while polyunsaturated fatty acids have been established as major stimuli for lipid droplet formation (27), it remains unknown what function these droplets have in cells that do not normally store large amounts of lipid, such as monocytes. In addition, a concise mechanism describing fatty acid uptake and repackaging into triglyceride-filled droplets by immune cells is unknown.

Previous research has shown that neutral lipid storage is important for cellular defense. Excess fatty acids are toxic to cells, but unsaturated fatty acids have been shown to protect normal cells against the damage induced by saturated fatty acids (28). One possible reason that lipid droplets form in response to VLDL lipolysis products is to prevent lipotoxicity, which has clinical relevance in human disease. The cellular mechanisms by which lipid-laden cells tolerate lipid overload or undergo lipotoxicity are not well known. Recently, Cnop et al. showed that pancreatic islet cells treated with oleate were able to survive lipotoxicity by forming lipid droplets, while cells that did not survive the treatment did not contain droplets (29). In our study, THP-1 monocytes formed lipid droplets in response to polyunsaturated, monounsaturated, and saturated fatty acids, while maintaining cell viability. In a previous study, we determined that lipolysis of VLDL from healthy individuals releases a combination of fatty acids of which palmitic acid (120 ± 19 nmol / mg TG), stearic acid (23.8 ± 6.3 nmol / mg TG), oleic acid (67.8 ± 10 nmol / mg TG), and linoleic acid (48.2 ± 11 nmol / mg TG) were the most abundant (22). Exposure of monocytes to this combination of saturated and unsaturated non-esterified fatty acids results in the formation of lipid droplets. We can speculate that the sequestration of long chain fatty acids into droplets prevents them from initiating pro-apoptotic signaling cascades and/or generating reactive oxygen species, two endpoints of lipotoxicity.

We have shown that the saturated fatty acid palmitic acid leads to the highest level of lipid droplet formation, but likely at the expense of long-term cell viability. Higa et al. showed that palmitate increased triglyceride accumulation in pancreatic β cells, presumably by forming lipid droplets, but this lipid accumulation was not linked to subsequent apoptosis at high palmitate concentrations (30). A continuous dose-dependent Akt phosphorylation in those cells suggests that the accumulated lipid droplets triggered cell survival pathways through Akt. However, at higher doses of palmitate the cells became apoptotic, suggesting that either lipid droplet-induced survival signaling can reach a threshold, or that the cells switched over to a pro-apoptotic pathway. Similarly, Listenberger et al. showed that CHO cells treated with palmitate did not accumulate triglyceride and became apoptotic, while cells treated with oleate did accumulate lipids and survived lipotoxicity (28). They reasoned that the accumulation of triglyceride protected the cells from apoptosis, implying that unsaturated fatty acids protect against lipotoxicity while saturated fatty acids promote it. In contrast, our study shows that lipid droplets form after monocyte treatment of both saturated and unsaturated fatty acids. It is possible that our treatment dose of 150 μ M, palmitic acid was able to accumulate in lipid droplets, while the higher treatment concentrations reported by Listenberger et al. yielded different results. Additionally, the treatment times varied, which could also explain the discrepancies between studies.

It has previously been reported that sites of inflammation inside the human body, such as arthritic joints or asthmatic bronchi, contain cells with lipid droplets (31,32). This suggests that lipid droplets may play a role in regulating or responding to inflammation. Previous results reported by Bozza et al. showed that lipid body formation could be inhibited by aspirin and non-steroidal anti-inflammatory drugs, indicating that cyclooxygenase-2 and its downstream eicosanoid and prostaglandin targets are involved (33). Cyclooxygenase-2 and prostaglandins also have been found inside lipid bodies from neutrophils, eosinophils, mast cells, and adenocarcinoma cell lines (34–36). Haversen et al. showed that long-chain fatty acids, such as palmitate and stearate, induced the mRNA expression and secretion of inflammatory mediators TNF α , IL-1 β , and IL-8 from monocyte-derived macrophages, but linoleate did not induce cytokine secretion (37). The fact that these two saturated fatty acids are abundantly released from hydrolysis of our VLDL, they both initiate lipid droplet formation, and have been shown to elicit an inflammatory response from monocyte-derived macrophages suggests that they are primary activating agents in our system. We have demonstrated herein that VLDL lipolysis products initiate a pro-inflammatory response from monocytes, which becomes attenuated when the stimulus to lipid droplet formation is blocked. An important question that remains is whether or not there is a cause-and-effect relationship between the monocyte pro-inflammatory state and droplet formation.

In an effort to determine the origin of lipid droplets in monocytes, we stained specific organelles to determine if they co-localize with lipid droplets present. Based on the comparison between fluorescence from these organelle-specific stains and DIC images, it appears that there is a time-dependent association with ER. Lipid droplets that originate from the ER may be too small to be captured by current microscopic techniques, and remain unassociated from the ER while they become large enough to detect (38). TEM images of VLDL lipolysis product-treated monocytes show lipid droplets in close proximity to the ER membrane. The notion that lipid droplets arise as specialized regions of the ER is attractive, given that in times of metabolic stress this would facilitate the rapid exchange of lipids and proteins. However, the possibility of an endosomal trafficking mechanism also exists regarding the formation of lipid droplets. Fatty acids have been shown to induce the internalization and endosomal association of caveolin-1 and fatty acid binding proteins, which normally reside in membrane regions termed caveolae (39,40). In addition, it has been shown that caveolin-1 associates with lipid droplets and can directly bind fatty acids (41), suggesting that the lipid droplet contents originate from outside of the cell, which could be the case in our study.

We observed profound effects on the overall lipid composition of lipid droplets after treatment with lipolysis products from fasting versus postprandial VLDL. The postprandial period, as experienced multiple times per day, is often characterized by increased levels of circulating triglycerides and fatty acids (42,43), and also by activated monocytes (3). As evidenced by Raman spectroscopic analyses of individual intracellular lipid droplets, exposure to lipolysis products from postprandial VLDL resulted in a higher level of saturation (15%) inside the lipid droplets, which is likely to invoke a stronger lipotoxic response. In support of this result, Chan et al. have shown that VLDL isolated from the same population of fasting subjects has a lower saturated fatty acid content than postprandial VLDL (24). Overall, our results suggest that a higher saturated to unsaturated fat ratio in postprandial VLDL contributes to increased monocyte lipid droplet formation during the peak postprandial period, potentially representing an activating event leading to monocyte recruitment to the vascular wall.

While the formation of lipid droplets in a monocyte cell line in response to VLDL lipolysis product exposure is an interesting observation, it was important to establish physiological relevance. By conducting a study with randomly selected healthy volunteers, we confirmed the presence of lipid droplets in their monocytes before and 3.5 hours after the consumption of a moderately high fat meal. We found that these subjects exhibited an increase in plasma

triglycerides 3–4 hours following meal consumption, as has been previously reported (43,44), and which coincides with the peak monocyte inflammatory response (3). We speculated that, as seen *in vitro*, elevated VLDL lipolysis products could induce lipid droplet formation within circulating monocytes *in vivo*. Here, we report for the first time that monocytes isolated from human subjects during the peak postprandial period contain lipid droplets. A similar finding has recently been reported in hypercholesterolemic apoE knockout mice (45), from which CD11c⁺ monocytes contained lipid droplets while the same monocytic population from wild-type mice did not. This monocytic response to a high fat meal could be even more pronounced in humans with dyslipidemias such as combined dyslipidemia.

In this study, we have conclusively determined that monocytes treated with postprandial VLDL lipolysis products generate droplets that are in fact lipid-filled, form due to interactions with free fatty acids, are likely to originate from the ER, and are found both *in vitro* and more importantly *in vivo*. Furthermore, we speculate that these lipid droplets form to prevent lipotoxicity. We have also established that both unsaturated and saturated fatty acids induce lipid droplet formation, but that the increased number of cells containing lipid droplets seen postprandially could be linked to a higher saturated to unsaturated fatty acid ratio in postprandial VLDL. The identification of lipid droplets inside human monocytes could provide a novel biomarker for stratification of risk for ASCVD in the future.

Supplementary Material

Refer to Web version on PubMed Central for supplementary material.

Acknowledgments

We thank JoAnne Engebrecht (University of California at Davis) and Satya Dandekar (University of California at Davis) for use of their microscopes to complete this work, as well as Grete Adamson and Patricia Kysar for technical assistance in the Electron Microscopy Laboratory, Department of Pathology and Laboratory Medicine, University of California at Davis. We also thank Gregory McNerny for technical assistance with the Delta Vision deconvolution microscope, and Tyler Weeks and Iwan Schie for help in acquiring monocyte CARS images.

Sources of support: We are grateful to our funding sources, including a graduate fellowship from the Center for Biophotonics Science and Technology in Sacramento, CA and NHLBI HL055667. This work was supported in part by funding for the American Heart Association through a Grant-in-Aid to T.H., and by the National Science Foundation. The Center for Biophotonics, and NSF Science and Technology Center, is managed by the University of California, Davis, under Cooperative Agreement No. PHY 0120999. Support is also acknowledged from the Clinical Translational Science Center under grant number UL1 RR024146 from the National Center for Research Resources (NCRR), a component of the National Institutes of Health (NIH), and the NIH Roadmap for Medical Research.

References

1. Kelley JL, Rozek MM, Suenram CA, Schwartz CJ. Activation of human peripheral blood monocytes by lipoproteins. *Am J Pathol* 1988;130:223–231. [PubMed: 3124626]
2. Alipour A, van Oostrom AJ, Izraeljan A, Verseyden C, Collins JM, Frayn KN, Plokker TW, Elte JW, Castro Cabezas M. Leukocyte activation by triglyceride-rich lipoproteins. *Arterioscler Thromb Vasc Biol* 2008;28:792–797. [PubMed: 18218988]
3. Hyson DA, Paglieroni TG, Wun T, Rutledge JC. Postprandial lipemia is associated with platelet and monocyte activation and increased monocyte cytokine expression in normolipemic men. *Clin Appl Thromb Hemost* 2002;8:147–155. [PubMed: 12121056]
4. Eiselein L, Wilson DW, Lame MW, Rutledge JC. Lipolysis products from triglyceride-rich lipoproteins increase endothelial permeability, perturb zonula occludens-1 and F-actin, and induce apoptosis. *Am J Physiol Heart Circ Physiol* 2007;292:H2745–H2753. [PubMed: 17259442]
5. Fujimoto T, Ohsaki Y, Cheng J, Suzuki M, Shinohara Y. Lipid droplets: a classic organelle with new outfits. *Histochem Cell Biol* 2008;130:263–279. [PubMed: 18546013]

6. Murphy DJ. The biogenesis and functions of lipid bodies in animals, plants and microorganisms. *Prog Lipid Res* 2001;40:325–438. [PubMed: 11470496]
7. Fujimoto T, Ohsaki Y. Cytoplasmic lipid droplets: rediscovery of an old structure as a unique platform. *Ann N Y Acad Sci* 2006;1086:104–115. [PubMed: 17185509]
8. Martin S, Parton RG. Lipid droplets: a unified view of a dynamic organelle. *Nat Rev Mol Cell Biol* 2006;7:373–378. [PubMed: 16550215]
9. Welte MA. Proteins under new management: lipid droplets deliver. *Trends Cell Biol* 2007;17:363–369. [PubMed: 17766117]
10. Murphy DJ, Vance J. Mechanisms of lipid-body formation. *Trends Biochem Sci* 1999;24:109–115. [PubMed: 10203758]
11. Brown DA. Lipid droplets: proteins floating on a pool of fat. *Curr Biol* 2001;11:R446–R449. [PubMed: 11516669]
12. Novikoff AB, Novikoff PM, Rosen OM, Rubin CS. Organelle relationships in cultured 3T3-L1 preadipocytes. *J Cell Biol* 1980;87:180–196. [PubMed: 7191426]
13. Tauchi-Sato K, Ozeki S, Houjou T, Taguchi R, Fujimoto T. The surface of lipid droplets is a phospholipid monolayer with a unique Fatty Acid composition. *J Biol Chem* 2002;277:44507–44512. [PubMed: 12221100]
14. Le Lay S, Dugail I. Connecting lipid droplet biology and the metabolic syndrome. *Prog Lipid Res* 2009;48:191–195. [PubMed: 19303902]
15. Cohn JS, Wagner DA, Cohn SD, Millar JS, Schaefer EJ. Measurement of very low density and low density lipoprotein apolipoprotein (Apo) B-100 and high density lipoprotein Apo A-I production in human subjects using deuterated leucine. Effect of fasting and feeding. *J Clin Invest* 1990;85:804–811. [PubMed: 2107210]
16. Kota RS, Ramana CV, Tenorio FA, Enelow RI, Rutledge JC. Differential effects of lipoprotein lipase on tumor necrosis factor-alpha and interferon-gamma-mediated gene expression in human endothelial cells. *J Biol Chem* 2005;280:31076–31084. [PubMed: 15994321]
17. Kota RS, Rutledge JC, Gohil K, Kumar A, Enelow RI, Ramana CV. Regulation of gene expression in RAW 264.7 macrophage cell line by interferon-gamma. *Biochem Biophys Res Commun* 2006;342:1137–1146. [PubMed: 16516165]
18. Listenberger LL, Brown DA. Lipid droplets. *Curr Biol* 2008;18:R237–R238. [PubMed: 18364222]
19. Ross R. Atherosclerosis—an inflammatory disease. *The New England journal of medicine* 1999;340:115–126. [PubMed: 9887164]
20. Osterud B, Bjorklid E. Role of monocytes in atherogenesis. *Physiol Rev* 2003;83:1069–1112. [PubMed: 14506301]
21. Greaves DR, Channon KM. Inflammation and immune responses in atherosclerosis. *Trends Immunol* 2002;23:535–541. [PubMed: 12401406]
22. Wang L, Gill R, Pedersen TL, Higgins LJ, Newman JW, Rutledge JC. Triglyceride-rich lipoprotein lipolysis releases neutral and oxidized FFAs that induce endothelial cell inflammation. *J Lipid Res* 2009;50:204–213. [PubMed: 18812596]
23. Plaisance EP, Grandjean PW, Judd RL, Jones KW, Taylor JK. The influence of sex, body composition, and nonesterified fatty acids on serum adipokine concentrations. *Metabolism*. 2009
24. Chan JW, Motton D, Rutledge JC, Keim NL, Huser T. Raman spectroscopic analysis of biochemical changes in individual triglyceride-rich lipoproteins in the pre- and postprandial state. *Anal Chem* 2005;77:5870–5876. [PubMed: 16159116]
25. Rinia HA, Burger KN, Bonn M, Muller M. Quantitative label-free imaging of lipid composition and packing of individual cellular lipid droplets using multiplex CARS microscopy. *Biophys J* 2008;95:4908–4914. [PubMed: 18689461]
26. Le TT, Duren HM, Slipchenko MN, Hu CD, Cheng JX. Label-free quantitative analysis of lipid metabolism in living caenorhabditis elegans. *J Lipid Res*. 2009
27. Fujimoto Y, Onoduka J, Homma KJ, Yamaguchi S, Mori M, Higashi Y, Makita M, Kinoshita T, Noda J, Itabe H, Takano T. Long-chain fatty acids induce lipid droplet formation in a cultured human hepatocyte in a manner dependent of Acyl-CoA synthetase. *Biol Pharm Bull* 2006;29:2174–2180. [PubMed: 17077510]

28. Listenberger LL, Han X, Lewis SE, Cases S, Farese RV Jr, Ory DS, Schaffer JE. Triglyceride accumulation protects against fatty acid-induced lipotoxicity. *Proc Natl Acad Sci U S A* 2003;100:3077–3082. [PubMed: 12629214]
29. Cnop M, Hannaert JC, Hoorens A, Eizirik DL, Pipeleers DG. Inverse relationship between cytotoxicity of free fatty acids in pancreatic islet cells and cellular triglyceride accumulation. *Diabetes* 2001;50:1771–1777. [PubMed: 11473037]
30. Higa M, Shimabukuro M, Shimajiri Y, Takasu N, Shinjyo T, Inaba T. Protein kinase B/Akt signalling is required for palmitate-induced beta-cell lipotoxicity. *Diabetes Obes Metab* 2006;8:228–233. [PubMed: 16448528]
31. Weinstein J. Synovial fluid leukocytosis associated with intracellular lipid inclusions. *Arch Intern Med* 1980;140:560–561. [PubMed: 6244798]
32. Triggiani M, Oriente A, Seeds MC, Bass DA, Marone G, Chilton FH. Migration of human inflammatory cells into the lung results in the remodeling of arachidonic acid into a triglyceride pool. *J Exp Med* 1995;182:1181–1190. [PubMed: 7595189]
33. Bozza PT, Payne JL, Morham SG, Langenbach R, Smithies O, Weller PF. Leukocyte lipid body formation and eicosanoid generation: cyclooxygenase-independent inhibition by aspirin. *Proc Natl Acad Sci U S A* 1996;93:11091–11096. [PubMed: 8855314]
34. Dvorak AM, Morgan E, Schleimer RP, Ryeom SW, Lichtenstein LM, Weller PF. Ultrastructural immunogold localization of prostaglandin endoperoxide synthase (cyclooxygenase) to non-membrane-bound cytoplasmic lipid bodies in human lung mast cells, alveolar macrophages, type II pneumocytes, and neutrophils. *J Histochem Cytochem* 1992;40:759–769. [PubMed: 1316915]
35. Dvorak AM, Morgan ES, Tzizik DM, Weller PF. Prostaglandin endoperoxide synthase (cyclooxygenase): ultrastructural localization to nonmembrane-bound cytoplasmic lipid bodies in human eosinophils and 3T3 fibroblasts. *Int Arch Allergy Immunol* 1994;105:245–250. [PubMed: 7920026]
36. Accioly MT, Pacheco P, Maya-Monteiro CM, Carrossini N, Robbs BK, Oliveira SS, Kaufmann C, Morgado-Diaz JA, Bozza PT, Viola JP. Lipid bodies are reservoirs of cyclooxygenase-2 and sites of prostaglandin-E2 synthesis in colon cancer cells. *Cancer Res* 2008;68:1732–1740. [PubMed: 18339853]
37. Haversen L, Danielsson KN, Fogelstrand L, Wiklund O. Induction of proinflammatory cytokines by long-chain saturated fatty acids in human macrophages. *Atherosclerosis* 2009;202:382–393. [PubMed: 18599066]
38. Hakumaki JM, Kauppinen RA. ¹H NMR visible lipids in the life and death of cells. *Trends Biochem Sci* 2000;25:357–362. [PubMed: 10916153]
39. Trigatti BL, Anderson RG, Gerber GE. Identification of caveolin-1 as a fatty acid binding protein. *Biochem Biophys Res Commun* 1999;255:34–39. [PubMed: 10082651]
40. Pol A, Martin S, Fernandez MA, Ingelmo-Torres M, Ferguson C, Enrich C, Parton RG. Cholesterol and fatty acids regulate dynamic caveolin trafficking through the Golgi complex and between the cell surface and lipid bodies. *Mol Biol Cell* 2005;16:2091–2105. [PubMed: 15689493]
41. Pol A, Martin S, Fernandez MA, Ferguson C, Carozzi A, Luetterforst R, Enrich C, Parton RG. Dynamic and regulated association of caveolin with lipid bodies: modulation of lipid body motility and function by a dominant negative mutant. *Mol Biol Cell* 2004;15:99–110. [PubMed: 14528016]
42. Karpe F. Postprandial lipoprotein metabolism and atherosclerosis. *J Intern Med* 1999;246:341–355. [PubMed: 10583705]
43. Chung BH, Hennig B, Cho BH, Darnell BE. Effect of the fat composition of a single meal on the composition and cytotoxic potencies of lipolytically-releasable free fatty acids in postprandial plasma. *Atherosclerosis* 1998;141:321–332. [PubMed: 9862181]
44. Karpe F, Steiner G, Olivecrona T, Carlson LA, Hamsten A. Metabolism of triglyceride-rich lipoproteins during alimentary lipemia. *J Clin Invest* 1993;91:748–758. [PubMed: 8450056]
45. Wu H, Gower RM, Wang H, Perrard XY, Ma R, Bullard DC, Burns AR, Paul A, Smith CW, Simon SI, Ballantyne CM. Functional role of CD11c⁺ monocytes in atherogenesis associated with hypercholesterolemia. *Circulation* 2009;119:2708–2717. [PubMed: 19433759]

Abbreviations

TG	triglyceride
VLDL	very low-density lipoprotein
LpL	lipoprotein lipase
ASCVD	atherosclerotic cardiovascular disease
ER	endoplasmic reticulum
DIC	differential interference contrast
CARS	coherent anti-Stokes Raman scattering
TEM	transmission electron microscopy
PBMC	peripheral blood mononuclear cells

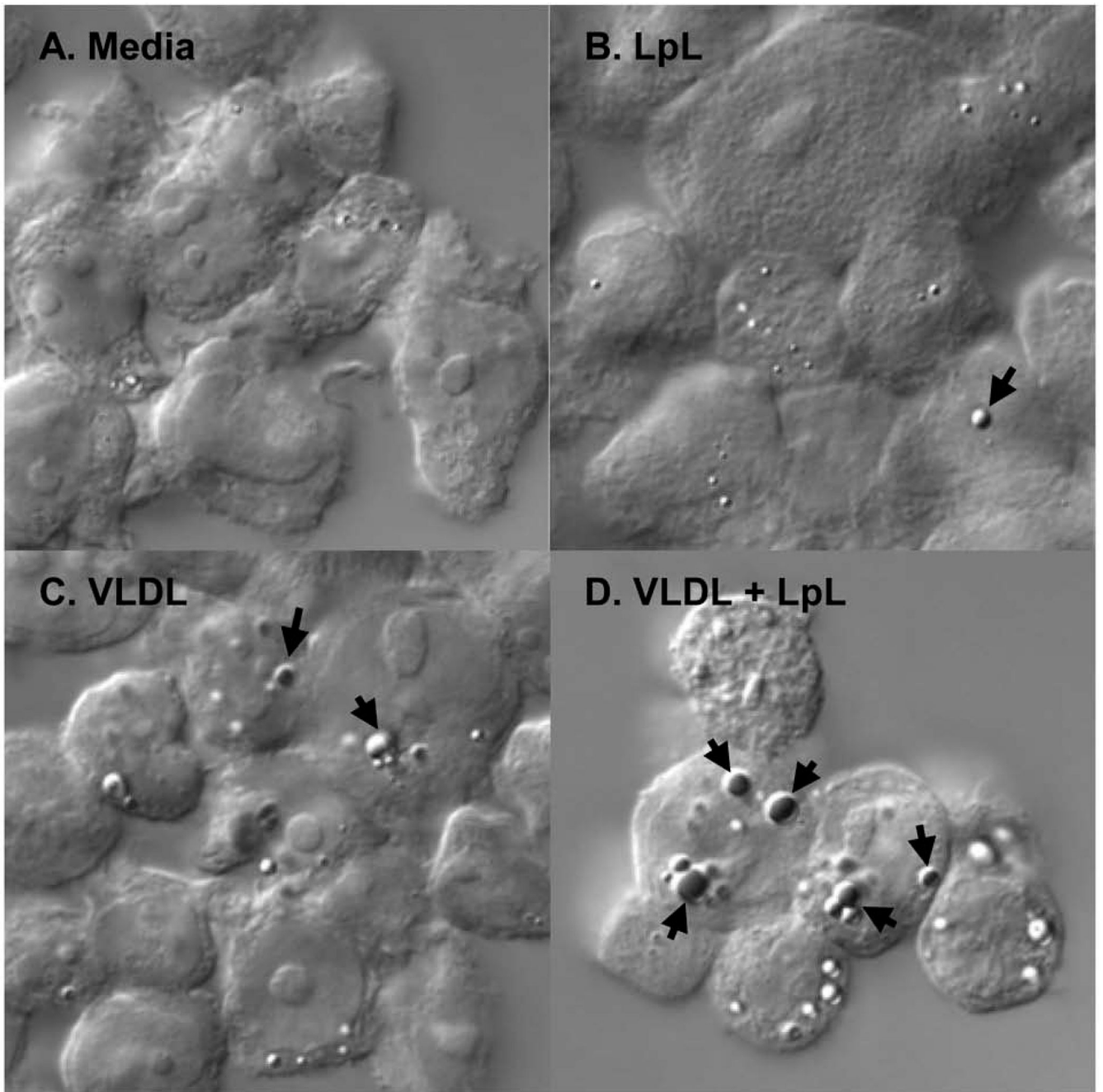


Figure 1. VLDL lipolysis product-induced droplets are lipid-filled

THP-1 monocytes were treated at a cell density of 1×10^6 cells/mL for 3 hours. Monocytes were fixed in 1% paraformaldehyde and lipid droplets were stained with Oil Red O. Monocytes were observed at room temperature using a Zeiss Axioskop2 plus microscope with a Pan-Neofluar 40 \times objective, 1.3 oil. DIC images were captured using a Zeiss AxioCam MRm camera and processed using AxioVision LE software. (A to C) Negative controls included (A) media, (B) LpL (2 U/mL), and (C) VLDL alone (200 mg TG/dL), and resulted in low levels of droplet formation. (D) VLDL lipolysis products (200 mg TG/dL VLDL + 2 U/mL LpL) induced formation of droplets that stained red with Oil Red O, indicating that they are lipid-filled. Cells from each treatment were analyzed over a minimum of 10 frames per experiment.

The experiment was repeated 3 times, with similar results. Arrows, lipid droplets. Original magnification $\times 400$ for panels A–D.

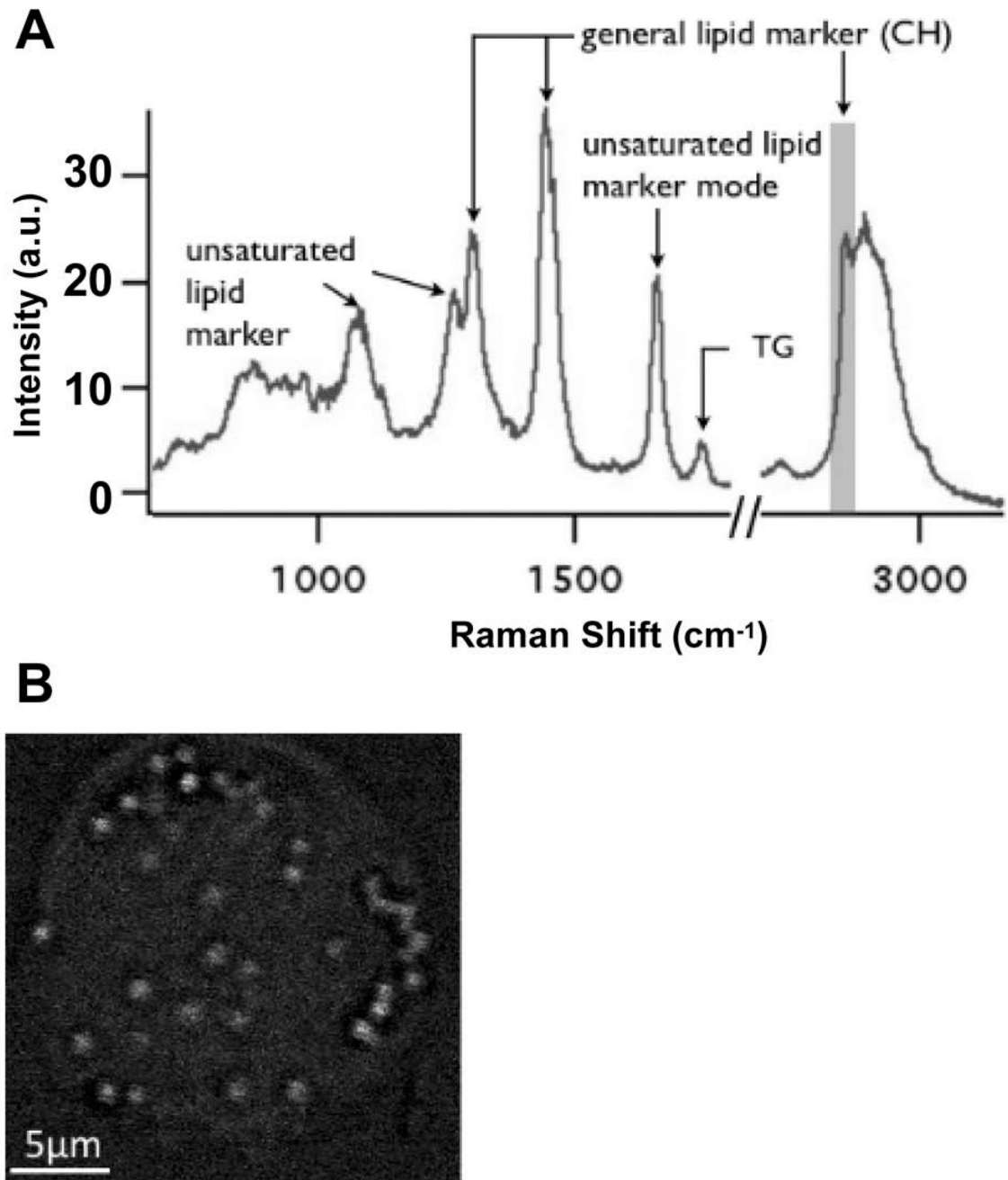


Figure 2. CARS imaging of THP-1 monocytes confirms the lipid nature of the droplets
 After a 3-hour treatment with VLDL + LpL (200 mg TG/mL, 2 U/mL), THP-1 monocytes were analyzed and imaged by CARS microscopy. (A) Raman spectra obtained from individual lipid droplets inside monocytes exhibit all the hallmarks of lipids. (B) A chemical image obtained by utilizing the general lipid marker mode of an aliphatic CH vibration at 2845 cm^{-1} to generate the contrast confirms that the droplets inside monocytes are highly enriched in lipids. Lipid droplets are $\sim 1 \mu\text{m}$ in diameter throughout the cell. Images and spectra were obtained on home-built instruments utilizing an Olympus I \times 71 inverted microscope as platform, equipped with an Olympus Plan-Apo 100 \times , 1.4 NA objective lens. Cells were fixed with 2% paraformaldehyde, washed in phosphate buffered saline, and imaged at room

temperature using Picoquant SymPhoTime software. $n = 3$; each replication represents the analysis of 5–8 fields of view. A.u., arbitrary units.

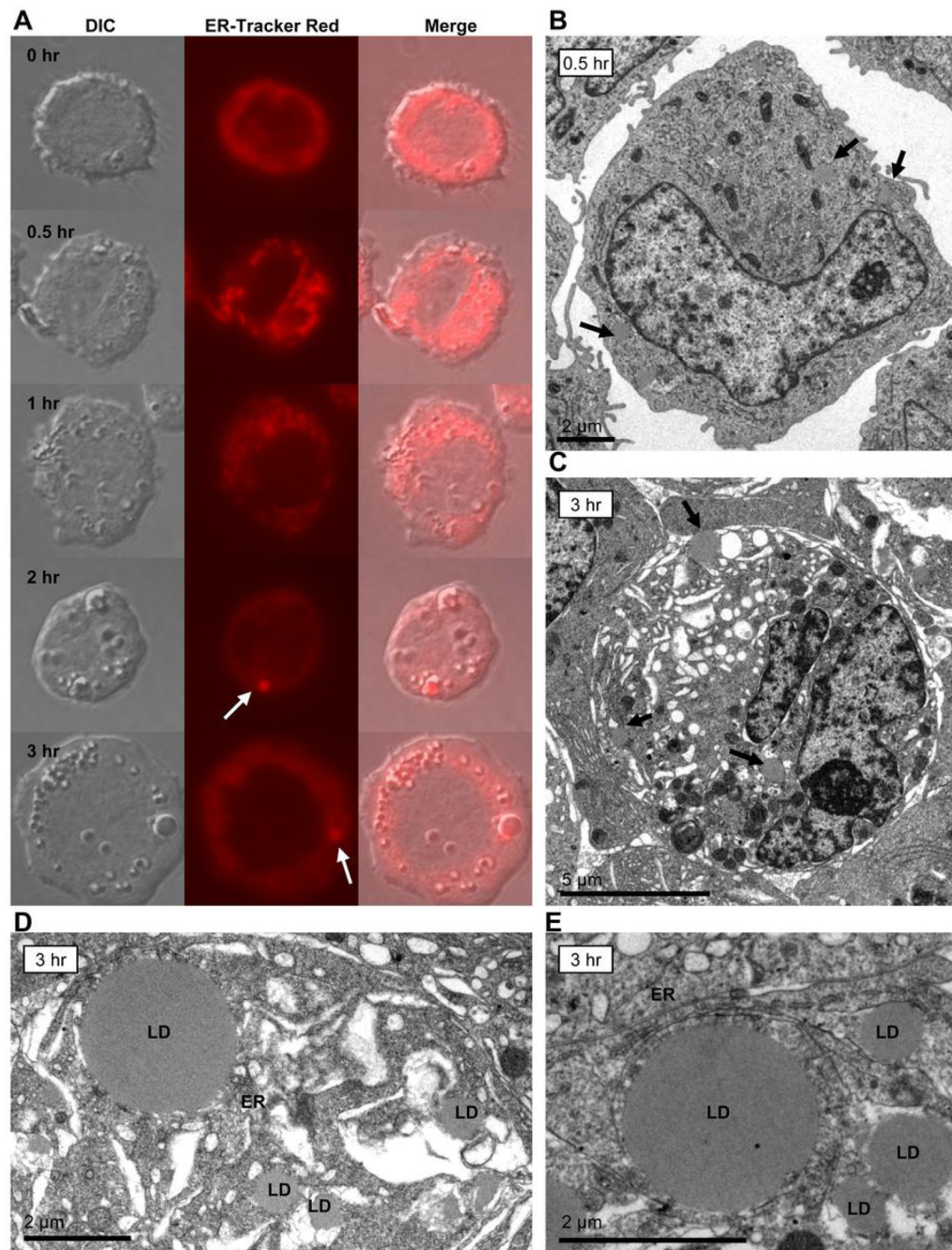


Figure 3. VLDL lipolysis product-induced lipid droplets are found in close proximity to the ER (A) THP-1 monocytes were treated at a cell density of 1×10^6 cells/mL with VLDL + LpL (200 mg TG/dL, 2 U/mL) over a time course ranging from 0.5 to 3 hours. At each time point cells were collected and stained with ER-Tracker Red to observe any interactions between ER structures and lipid droplet formation. Monocytes were observed using a Zeiss Axioskop2 plus microscope with a Pan-Neofluar 40 \times objective, 1.3 oil. Images were captured using a Zeiss AxioCam MRm camera and processed using AxioVisionLE software. Fluorescence and DIC images of the same cells are shown. At 2 hours, ER-associated contents are seen in the same area as some of the lipid droplets within the cell (ER-Tracker Red, arrow). By 3 hours, the ER appears to surround the lipid droplet and/or its contents (arrow). Cells from each treatment

were analyzed over a minimum of 10 frames per experiment. The experiment was repeated 3 times, with similar results. (B to E) TEM of THP-1 monocytes treated with VLDL + LpL (200 mg TG/dL, 2 U/mL) for either 0.5 or 3 hours. Monocytes were harvested, prepared for TEM analysis, and embedded in epoxy resin for ultra thin sectioning. The images were collected on a Phillips CM120 microscope at 80kV using a Gatan MegaScan model 794/20 digital camera. (B) Monocyte treated with VLDL lipolysis products for 0.5 hours contains small, disperse lipid droplets (original magnification $\times 8510$, arrows). (C) Monocyte treated with VLDL lipolysis products for 3 hours contains larger lipid droplets (original magnification $\times 8510$, arrows). (D and E) Higher magnification images of monocytes treated with VLDL lipolysis products for 3 hours reveal lipid droplets of multiple sizes (D, original magnification $\times 15900$) and lipid droplets in close proximity to the ER (E, original magnification $\times 11000$). LD, lipid droplet; ER, endoplasmic reticulum.

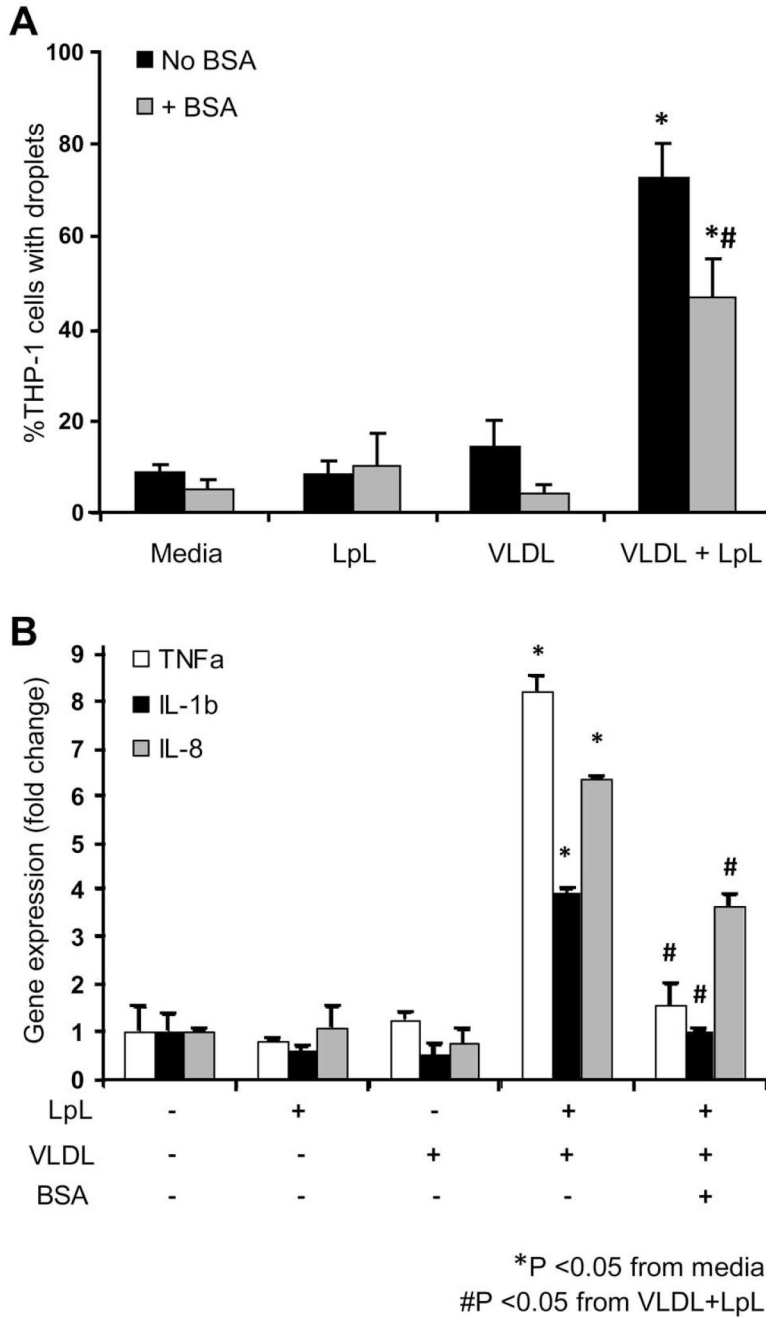


Figure 4. Binding fatty acids with BSA partially attenuates lipid droplet formation in THP-1 monocytes

Lipolysis of VLDL was allowed for 30 minutes at 37°C, fatty acid-free BSA was added for 5 minutes, then the combined treatment was applied to THP-1 monocytes for 3 hours. (A) Monocytes were fixed, stained with Oil Red O, and imaged by phase contrast microscopy using a 60× objective. Monocytes treated with media, LpL (2 U/mL), and VLDL (200 mg TG/mL) with and without BSA (60 mg/mL) were used as negative controls. Cells positive for lipid droplets in each treatment were counted, and expressed as a percentage of cells containing lipid droplets, n = 5. A minimum of 300 cells were counted for each treatment. (B) Gene expression of cytokines TNFα, IL-1β, and IL-8 measured from THP-1 monocytes treated with the above

treatments, normalized to media treatment and presented as fold change \pm SEM. *Values are significantly different from media control, $P < 0.05$. #Values are significantly different from the VLDL + LpL treatment without BSA, $P < 0.05$.

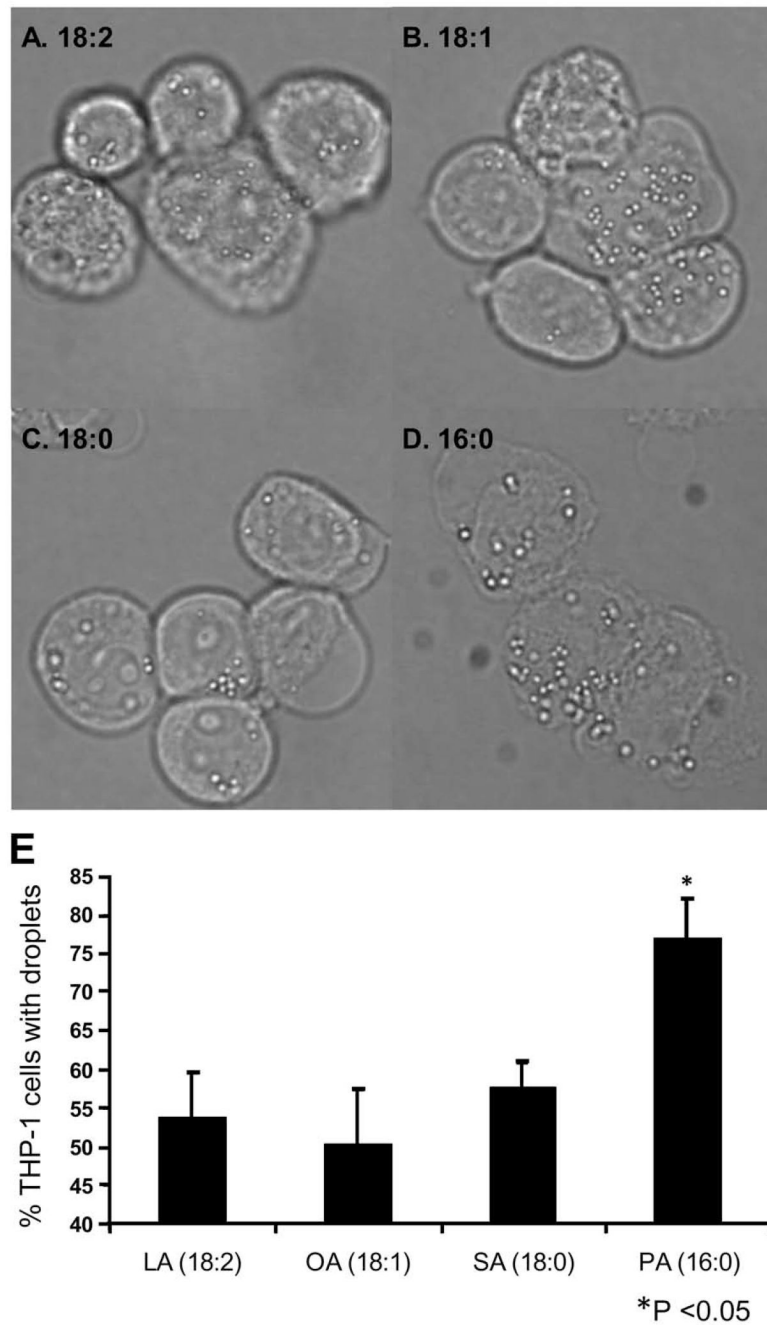


Figure 5. Synthetic fatty acids induce formation of lipid droplets in THP-1 monocytes
 THP-1 monocytes were treated at a cell density of 1×10^6 cells/mL with linoleic acid (A, LA (18:2), η -6), oleic acid (B, OA(18:1)), stearic acid (C, SA(18:0)), or palmitic acid (D, PA(16:0)) at final concentrations of 150 μ M for 3 hours. Monocytes were observed by phase contrast microscopy using an Olympus B \times 41 microscope with a 60 \times objective, NA 0.80. Images were captured using an Olympus QColor3 camera and processed using QCapture software. A minimum of 300 cells were counted from each treatment, and the average percentage of cells positive for lipid droplets is represented in panel E ($n = 3$, $*P < 0.05$). Original magnification $\times 600$ for all panels.

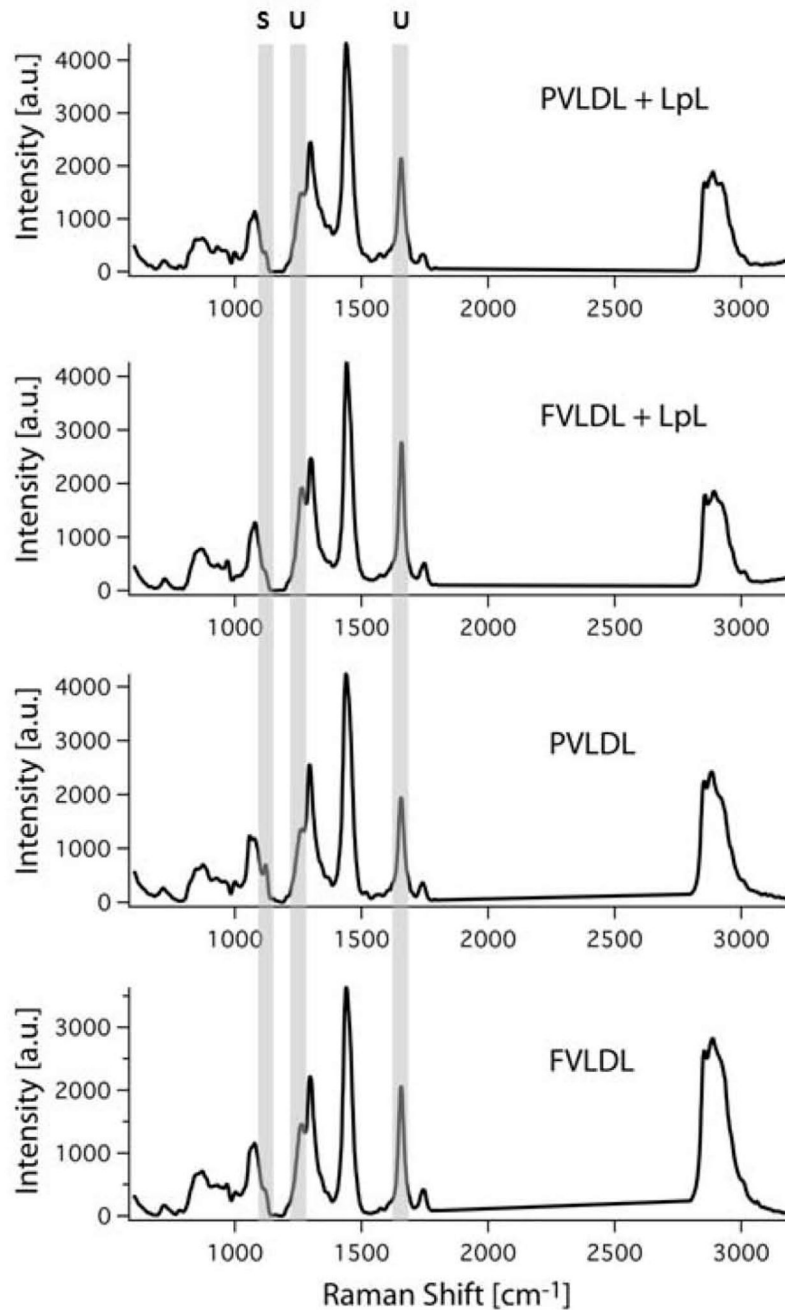


Figure 6. Lipid droplets in THP-1 monocytes exposed to fasting or postprandial VLDL lipolysis products exhibit distinct differences in their lipid composition

THP-1 monocytes were treated at a cell density of 1×10^6 cells/mL with either VLDL or VLDL + LpL (200 mg TG/dL, 2 U/mL) for 3 hours with VLDL obtained in the fasting (F) and the postprandial (P) states. THP-1 monocytes were also treated with F-VLDL and P-VLDL alone (in the absence of LpL). On average, 10 Raman spectra from cells treated with the different products were obtained and their signal intensities were averaged ($n = 3$). Raman markers for saturation (S, 1129 cm^{-1}) and unsaturation (U, 1266 cm^{-1} and 1654 cm^{-1}) are highlighted by grey bars. A.u., arbitrary units.

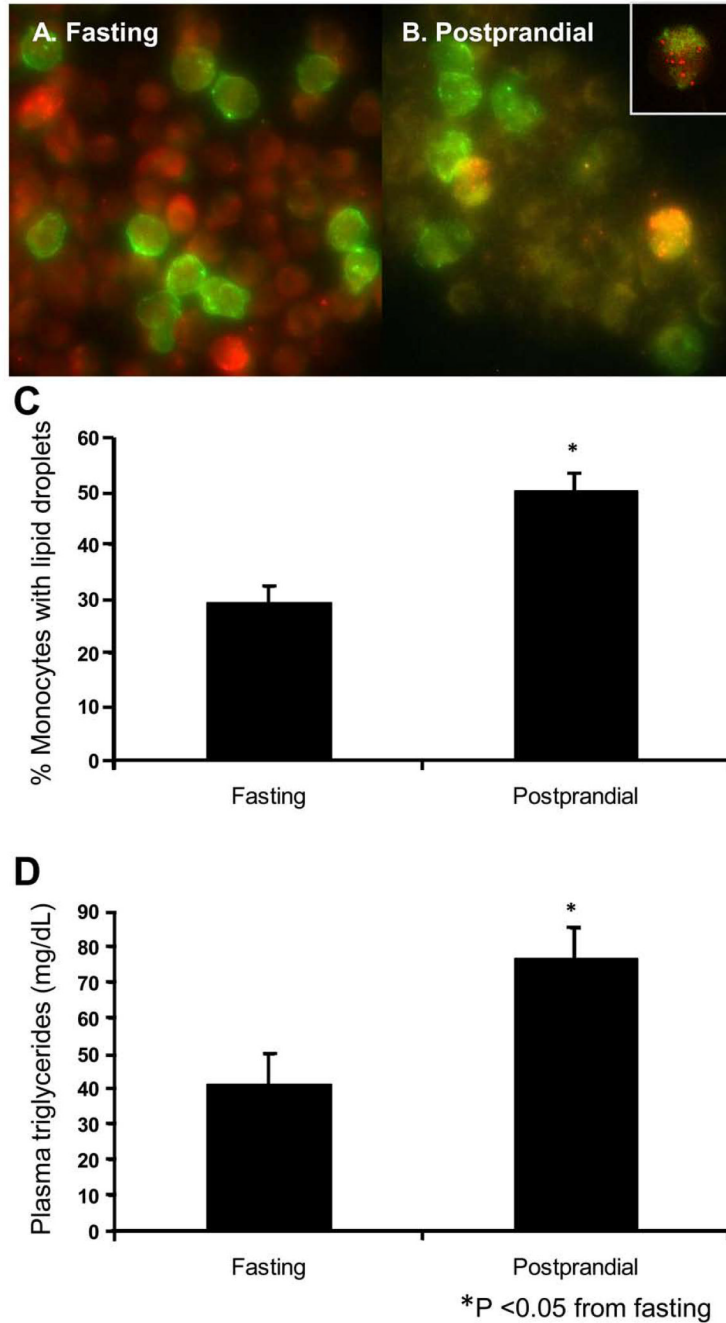


Figure 7. The postprandial state induces lipid droplet formation in freshly isolated human monocytes

(A to B) Peripheral blood was drawn before and after consumption of a moderately high fat meal from 10 healthy human volunteers. Monocytes were labeled with CD14-FITC, fixed, and stained with Oil Red O. (A) Fasting and (B) postprandial monocytes were imaged using a Delta Vision Deconvolution microscope with a 60× objective. CD14-positive monocytes are shown in green, while Oil Red O-stained lipid droplets appear red. (Inset of panel B) A CD14-positive monocyte that contains lipid droplets is shown at 2× digital magnification. (C) Percent cells containing lipid droplets was calculated by analyzing 40 frames from each sample, with a minimum of 150 cells counted from each fasting and postprandial time point for each subject.

50.3 ± 3.1% of postprandial monocytes contained lipid droplets, compared to 29.4 ± 3.0% of monocytes during the fasting state. (D) Postprandial blood plasma triglyceride levels (77.0 ± 8.3 mg TG/dL) were also higher compared to fasting blood samples (41.5 ± 8.3 mg TG/dL), averaged from 10 subject samples. *P<0.05. Original magnification ×600 for panels A–B.